Research Square

Preprints are preliminary reports that have not undergone peer review.
They should not be considered conclusive, used to inform clinical practice,
or referenced by the media as validated information.

Finite element simulation study of pipe structure damage based on rough surface parameters

Ying Li
University of Emergency Management
ZeCan Chen
University of Emergency Management
Jia Wei
paper20152025@163.com

University of Emergency Management

Article

Keywords: Surface roughness parameter; Damage index matrix; Wavelet decomposition method, Guided wave torsion

Posted Date: March 12th, 2026

DOI: https://doi.org/10.21203/rs.3.rs-9003270/v1

License: This work is licensed under a Creative Commons Attribution 4.0 International License.
Read Full License

Additional Declarations: No competing interests reported.

Finite element simulation study of pipe structure damage based on rough surface parameters

Ying Li [1, 2,] ZeCan Chen[1, 2,] Jia Wei[1,2,] *

[1]Hebei Technology Innovation Center for Multi-Hazard Resilience and Emergency Handling of Engineering Structures, San he, 065201, China;

[2] University of Emergency Management, School of Earthquake Engineering and Building Safety, San he, 065201, China;

*Correspondence: paper20152025@163.com

ABSTRACT

This paper investigates the correlation between single parameters of pipeline damage (i.e., central angle, axial width, and surface roughness) and damage index values, treating surface roughness as a key characteristic parameter for modeling damaged surface morphology. First, a rough surface damage model was established using Gaussian distribution parameters based on ABAQUS finite element software. Subsequently, pipe finite element models with varying damage center angles, axial widths, and surface roughness parameters were constructed. Damage index values were calculated by extracting piezoelectric signals and performing wavelet packet decomposition, followed by analysis of the variation patterns in the damage index matrix. The study revealed that, with other parameters held constant, the damage index monotonically increases with the damage central angle. However, it exhibits a non-monotonic trend—first decreasing and then increasing—with increases in damage axial width and surface roughness. Based on the fitting curve between the damage index and the severity of roughness-corrosion damage, the damage level can be rapidly identified and its development trend predicted. Furthermore, incorporating the surface roughness parameter enhances the realism of the damage model, providing a reliable finite element analysis method for pipeline damage diagnosis based on surface morphology.

Keywords: Surface roughness parameter; Damage index matrix; Wavelet decomposition method; Guided wave torsion.

Introduction

Pipelines are widely used for transporting petroleum, natural gas, water, and other media due to their advantages of short transport distances, minimal terrain constraints, and non-occupancy of surface space. In engineering applications, pipeline structures are prone to various damages during long-term service due to factors such as corrosion, fatigue, or external impacts. The damaged surfaces are non-smooth, and quantitative detection of damage depth is crucial for determining pipeline operational safety. Ultrasonic guided waves, characterized by weak dispersion effects and long-distance propagation capabilities, are commonly employed for pipeline damage detection. This paper employs ABAQUS finite element analysis software to simulate guided wave propagation characteristics within

pipeline structures. Concurrently, wavelet packet decomposition is applied to analyze received signal features. Ultimately, pipeline rough surface damage identification is achieved based on a damage index matrix. In the field of pipeline non-destructive testing, torsional guided waves not only exhibit high sensitivity to circumferential damage but also possess the capability to detect axial damage and feature low attenuation characteristics [1]. These properties make them particularly suitable for comprehensive detection of various defect types in long pipelines. Therefore, torsional guided waves were selected as the detection modality in this study.

In the field of signal processing and structural damage identification based on wavelet packet decomposition, Du Guofeng et al. [2] identified the damage severity of pipeline cracks under external load impact. They applied the wavelet packet energy formula to calculate the energy of sensor signals from both healthy and damaged pipelines, then computed the damage index based on the root mean square deviation. They further explored the feasibility of pipeline damage identification by analyzing changes in the damage index. Wang et al. [3] analyzed the relationship between damage parameters and damage indices in fluid-filled pipelines, proposing a rapid damage severity identification method. PAN et al. [4] conducted damage detection experiments on single-layer fluid-filled pipelines. This method first performs wavelet decomposition and reconstruction on the received signal, then achieves damage localization based on the reconstructed signal, enhancing localization accuracy. LANG et al. [5] proposed a leakage hole identification method for oil pipelines that integrates wavelet packet decomposition, deep belief networks (DBN), and independent component regression. Experiments demonstrate this method can rapidly and effectively identify different leak apertures. This study avoids direct reflection coefficient measurement by adopting a novel approach: wavelet packet decomposition extracts a quantized damage index highly sensitive to energy distribution changes from complex sensor signals. Wavelet packet decomposition precisely separates signal energy components across different frequency bands. The propagation of circumferential defects systematically disturbs this frequency-band energy distribution. Consequently, this study introduces a highly sensitive quantitative assessment parameter based on energy-band analysis. It successfully correlates three geometric parameters—damage center angle, axial width, and surface roughness—with the damage index as a quantitative metric. This provides a more precise model and basis for quantitative damage assessment in pipelines using piezoelectric guided waves.

Previous studies typically simplified damage into idealized smooth surface models, neglecting the actual surface roughness of pipelines caused by factors such as corrosion, machining, or wear. This idealized assumption may lead to discrepancies between simulation results and real-world conditions. In recent years, increased attention has been directed toward the morphology of damaged surfaces. Feng Qibo et al. [6] emphasized the concept of surface roughness parameters and provided a detailed introduction to both contact and non-contact measurement methods; Lü Zhiyang et al. [7] analyzed the impact of varying roughness on contact stress using finite element software. Such research focuses on characterization parameters for actual rough surfaces, reflecting the surface roughness morphology of pipeline structures under real operating conditions. Additionally, the team led by Kang Yihua [8] systematically analyzed the impact of surface roughness on ultrasonic wave propagation and verified the influence of workpiece surface roughness on the measurement accuracy of piezoelectric ultrasonic thickness gauges. This paper employs a rough surface randomly generated based on the Gaussian height probability density distribution function to realistically simulate actual corrosion morphology. By controlling the statistical distribution (e.g., Gaussian distribution) and variance (Ra) parameters of surface height, flexible and

quantitative modeling of damage with varying roughness levels was achieved. This method establishes a physical model that better aligns with industrial realities and quantitatively describes surface microgeometric morphology.

To this end, ABAQUS software was employed to excite torsional guided waves propagating within the pipeline. Combined with wavelet packet decomposition, a damage index matrix was constructed. By calculating damage indices corresponding to rough surface damage with varying circular angles, axial widths, and surface roughness levels, the corresponding damage index fitting curves were obtained. Establishing a linear fitting relationship between rough surface damage depth and damage index enabled damage severity identification and prediction of future damage trends.

Theoretical Basis

Twisted Wave Theory

In an isotropic, uniform, elastic, infinitely long circular pipe (as shown in Figure 1), assuming that a time harmonic wave propagates along the pipe, the displacement u and shear force τ of the torsional guided wave [9] in the pipe are expressed as follows:

$$u_\theta = [AZ_1(qr) + BW_1(qr)]\, e^{i(\omega t - kz)} \quad (1)$$

$$\tau_{r\theta} = -\mu q\, [AZ_2(qr) + BW_2(qr)]\, e^{i(\omega t - kz)} \quad (2)$$

In the equation, A and B are constants, c_T is the transverse wave velocity of the material, $c_T^2 = \mu/\varrho$, μ is the shear modulus of the material, k is the axial wave number, ω is the angular frequency, and r is the radius. In the equation, Zn and Wn are a pair of linearly independent Bessel functions, e is the natural logarithm, and $q^2 = \omega^2/c^2T - k^2$.

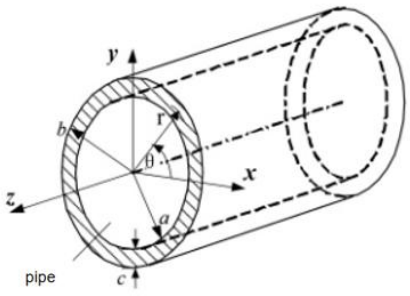


Figure 1. Pipeline structure.

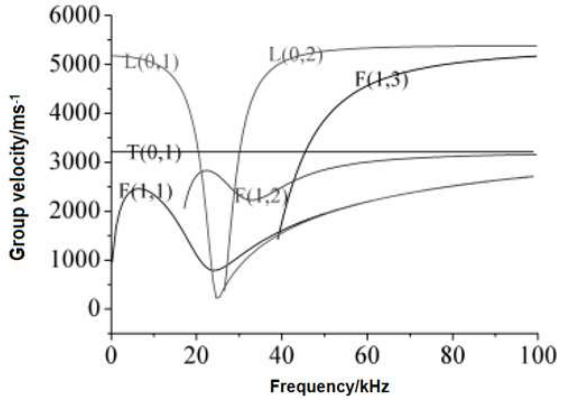


Figure 2. Dispersion curve.

This paper is based on torsional modal guided waves, which are highly sensitive to both circumferential and axial damage and exhibit a non-dispersive region with relatively high propagation velocity within the 0 to 100 kHz frequency range. The dispersion curves of torsional guided waves in pipe structures were calculated using MATLAB. Figure 2 displays the group velocity dispersion curve for torsional modes in a steel pipe with an outer diameter of 76 mm and a wall thickness of 4 mm, where the theoretical wave velocity is 3182 m/s.

Damage Index

Du [2] et al. established a damage index matrix based on wavelet packets, and the energy and damage index value I of each signal subset are expressed by the following formulas

$$E_j = \sum_{k=1}^{k=m} X_{j,k}^2 \tag{3}$$

$$I = \sqrt{\frac{\sum_{j=1}^{2^n} \left(E_{i,j} - E_{0,j}\right)^2}{\sum_{j=1}^{2^n} E_{0,j}^2}} \tag{4}$$

In the equation: i represents the time index corresponding to different measurement values; represents the energy of the jth subset signal under the undamaged structural state; represents the energy of the jth subset signal at the ith time index under the damaged structural state.

Based on the obtained damage index values, within the two-dimensional damage index matrix system, the x-axis represents the damage condition number, while the y-axis corresponds to the damage index value. By constructing the damage index matrix based on the damage severity gradient, the mapping relationships between the damage index and parameters such as the damage center angle, axial width, and surface roughness can be analyzed separately, thereby enabling damage identification. This method not only quantifies the influence of different damage parameters on damage severity but also visually demonstrates the damage evolution patterns under multifactorial effects through the coupling relationships among matrix parameters.

This study employs the MATLAB platform, utilizing the db5 wavelet basis function to perform a five-layer decomposition of the acquired signal (as shown in Figure 3) [10], ultimately yielding 32 feature signal components. In pipeline non-destructive testing, piezoelectric guided waves are susceptible to interference from multiple physical factors and phenomena such as modal conversion, leading to reduced signal-to-noise ratio in the acquired signals. In actual operating conditions, the rough morphology of damaged surfaces significantly exacerbates this signal degradation, making it difficult to accurately identify damage features based on raw potential signals. Wavelet packet decomposition technology can effectively process complex signals caused by such rough damaged surfaces. This is manifested in simultaneous decomposition across high and low frequency bands, offering superior resolution capabilities.

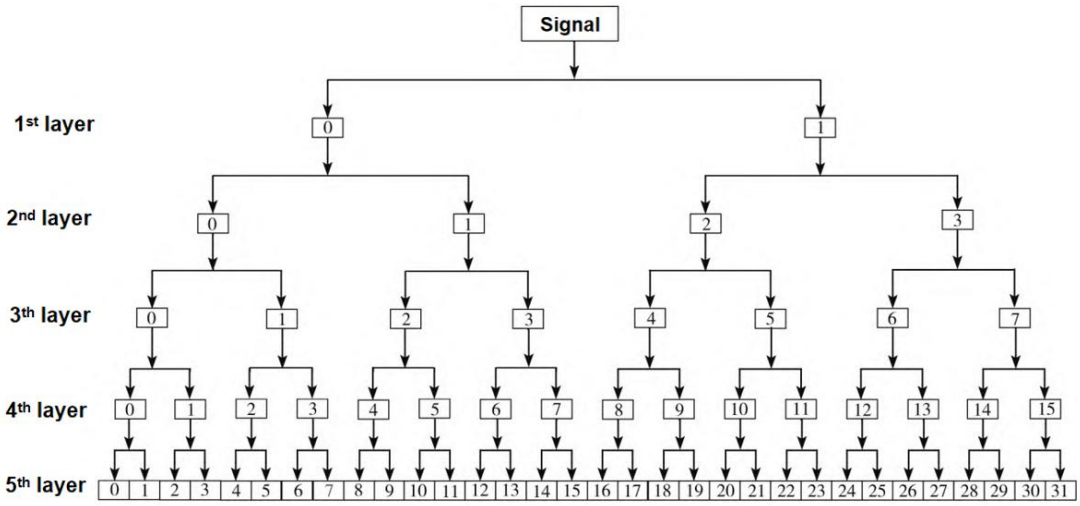


Figure 3. Five-layer wavelet packet decomposition tree.

Rough Surface Modeling

Typically, surface topography features smaller than 1 mm are attributed to surface roughness. To accurately characterize the roughness of damaged surfaces, this study employs the RufGen plugin [11] for ABAQUS finite element software to construct a surface roughness model. This plugin enables rapid parametric modeling of damaged surface topography by importing predefined damage patch models and configuring roughness parameters (e.g., height distribution, correlation length). The generated rough surface is then integrated into the overall pipe finite element model, allowing more realistic simulation of damaged corrosion surfaces under actual operating conditions.

Gaussian Distribution Modeling Principle: First, define the dimensions of the damage patch (length L_x and width L_y) in the x-y plane, uniformly distribute sampling points, and set the number of sampling points N_x and N_y. Then, sample according to the Gaussian distribution's Probability Density Function (PDF) to generate a z-axis coordinate (height value) for each sampling point. The schematic diagram of the rough surface morphology generated through the above steps is shown in Figure 2/4. Its mathematical model can be expressed as:

$$\text{Gaussian, } f(z)=\frac{1}{\sigma\sqrt{2\pi}}e^{-\frac{1}{2}(\frac{z}{\sigma})^2} \quad (5)$$

For the selection of surface roughness variance parameters, consideration must be given to the typical order of magnitude of pipe corrosion surface roughness encountered in practical engineering applications. This parameter range is established to systematically investigate the influence of continuous variations from near-smooth surfaces to highly rough surfaces on guided wave propagation. ASME B46.1 - Surface Texture (Surface Roughness, Waviness, and Lay) [12], five distinct surface roughness parameter ranges are established (5×10^{-5} to 25×10^{-5}).

The input parameters of the virtual rough surface in Figure 4 are shown in Table 1.

L_x/m	L_y/m	L_z/m	N_x	N_y	σ
0.012	0.004	0.001	18	6	0.00025

Table 1. Gaussian height distribution parameter

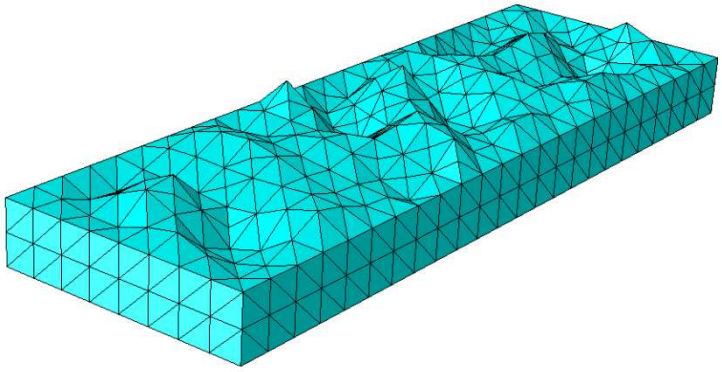


Figure 4. Rough surface diagram.

Numerical Simulation Design

Structural Model Construction Methods

A pipe model was established using ABAQUS finite element software. The pipe has an outer diameter of 76 mm, a wall thickness of 4 mm, and a length of 2000 mm. Piezoelectric elements made of piezoelectric ceramic (PZT) were selected, with dimensions of 12 mm × 6 mm × 1 mm (length × width × height). Material properties are shown in Table 2. To effectively excite the target mode while suppressing other unwanted modes (such as flexural modes), an exciter comprising 16 piezoelectric elements was positioned 30 mm from the pipe end. A receiver consisting of 4 piezoelectric elements was placed 300 mm from the pipe end in the same direction. This arrangement ensures that the guided wave at the excitation point is a torsional mode (T) wave while suppressing the generation of flexural mode (F) waves.

Material parameters/unit	Value					
Dielectric constant/(F/m)	D11	8.11E-09	D22	7.35E-09	D33	8.11E-09

Elastic constant /(N/m²)	D1111	1.21E+11	D1122	7.52E+10	D2222	1.11E+10
	D1133	7.54E+10	D2233	7.52E+10	D3333	1.21E+10
	D1212	2.11E+10	D1313	2.26E+10	D2323	2.11E+10
Piezoelectric constant/cm⁻²	e1 12	12.3	e2 11	-5.4	e3 23	12.3
	e2 22	-5.4	e2 33	15.8		

Table 2. Material parameters of piezoelectric elements

Design of Different Operating Condition Models

Among various types of pipeline damage, circumferential damage is particularly significant due to its impact on the pipeline's load-bearing capacity and structural integrity, making it highly representative. Therefore, research on circumferential pipeline damage holds important theoretical value and engineering significance.

For the selection of detection guided waves, this paper employs torsional guided waves (T-mode). This choice is based on torsional guided waves' high sensitivity to both axial and circumferential pipeline damage, enabling effective capture of signal characteristics induced by damage. The specific locations and arrangements of circumferential damage are illustrated in Figure 5.

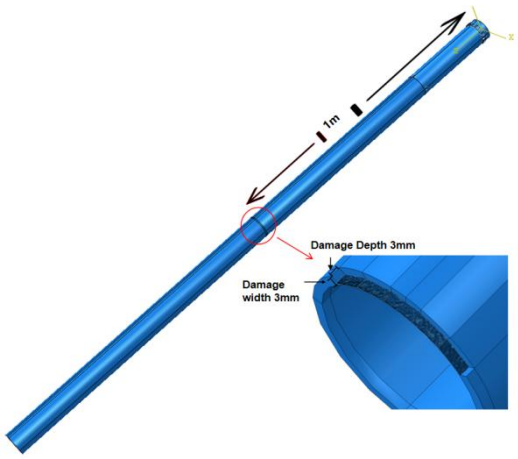


Figure 5. Detail of circumferential damage.

To investigate the variation of the damage index I with individual damage geometric parameters (central angle, axial width, and surface roughness), thereby enabling predictive assessment of damage progression trends, a series of pipe finite element models with varying central angles, axial widths, and surface roughness must be established.

1) Operating Condition X (Central Angle Variable): The fixed damage parameters are a radial depth of 3 mm, axial width of 4 mm, and surface roughness standard deviation of 10×10^{-5}. The central angle of the damage increases incrementally in 20° steps. This condition investigates the influence of central angle variation on the damage index.

2) Operating Condition Y (Axial Width Variable): The damage's central angle is fixed at 40°, with a radial depth of 3 mm and a surface roughness standard deviation of 10×10^{-5}. The

axial width is incremented sequentially in 1 mm steps. This condition investigates the impact of axial width variation on the damage index.

3) Operating Condition Z (Roughness Variable): With fixed damage parameters of radial depth 2 mm, central angle 60°, and axial width 4 mm, the surface roughness standard deviation is incremented in steps of 5×10^{-5} This condition investigates the effect of surface roughness variation on the damage index. Based on the damage parameters from these three dimensions, the summary of operating conditions for the established pipeline finite element model is shown in Table 3.

Parameter	X、Y and Z operating conditions					
Operating condition	Healthy	X1	X2	X3	X4	X5
Radius angle/degree	0	20°	40°	60°	80°	100°
Operating condition	Healthy	Y1	Y2	Y3	Y4	Y15
Axial width /mm	0	1mm	2mm	3mm	4mm	5mm
Operating condition	Smooth	Z1	Z2	Z3	Z4	Z5
Roughness/Std Dev	0	5×10^{-5}	10×10^{-5}	15×10^{-5}	20×10^{-5}	25×10^{-5}

Note:

For **X** (Radius angle variation:20° to 100°), depth × width×Std Dev =3mm×4mm×10×10^{-5};

For **Y** (Axial width variation:1mm to 5mm), depth × angle ×Std Dev =3mm×4mm×10×10^{-5};

For **Z** (Roughness standard deviation variation:5×10^{-5} to 25×10^{-5}), depth × angle ×width=2mm× 60° × 4mm.

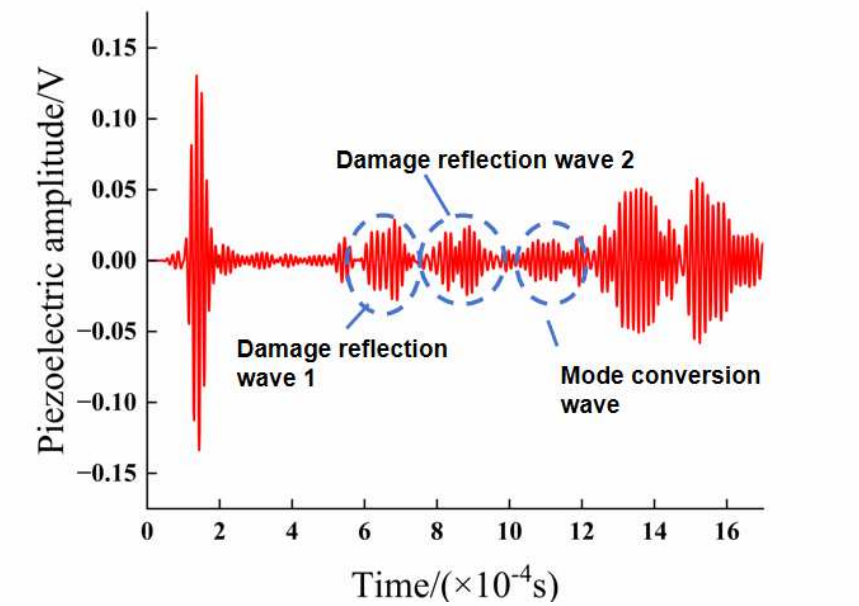
Table 2. Ultimate Tensile Strain Under Different Standards and Specifications.

Analysis of Simulation Test Results

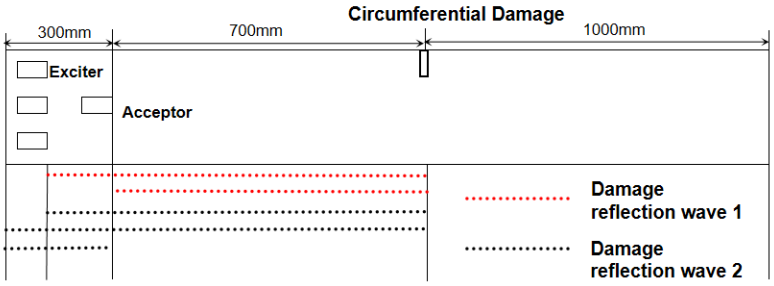
A Priori Analysis of Torsional Guided Wave Velocity

Under operating condition X3, the accuracy of the model was verified by analyzing the sensor signals received by the piezoelectric sensors, employing a comprehensive approach that combined numerical simulation with theoretical analysis comparisons and cross-referencing with experimental results from the literature. To validate the correctness of the finite element model in this study, experiments with identical parameter settings from He Binbin [13] were selected for comparison. These included: identical pipeline material properties, identical T (0,1) modal guided wave excitation parameters, a center frequency of 70 kHz, a Hann window of 10 periods, and identical circumferential damage geometry dimensions.

1) Wave velocity verification: The voltage signal at the receiver end was processed using wavelet packet decomposition (Figure 6a). The actual propagation velocity of the guided wave in the model, measured using the pulse-echo method, was 3131 m/s. This value exhibits a relative deviation of 1.63% from the theoretical group velocity of 3182 m/s and a relative deviation of 2.43% from the experimentally measured wave velocity of 3207 m/s reported in He Binbin [13].



(a) time domain diagram



(b) Dissemination routec

Figure.6 X3 working condition time domain diagram and propagation

2) Time-domain signal analysis: The actual arrival time of the damage reflection wave signal was 0.530×10^{-4} s. Compared to the theoretical arrival time (0.521×10^{-4} s), the relative time error was 1.63%; compared to the experimental value in Reference [13] (0.514×10^{-4} s), the relative error was 3.02% (Figure 6b).

3) Validation Conclusions: The consistency of boundary reflection wave velocity (relative error ≤ 2.43%) and the matching of damage echo spatio-temporal localization (relative error ≤ 3.02%) both fall within the <5% error range. This demonstrates the numerical accuracy and computational reliability of the established finite element model.

Indicators	Theoretical	Experimental	Numerical	Error (Theoretical)	Error (Experimental)
Propagation speed	3182 m/s	3207m/s	3131m/s	1.63%	2.43%

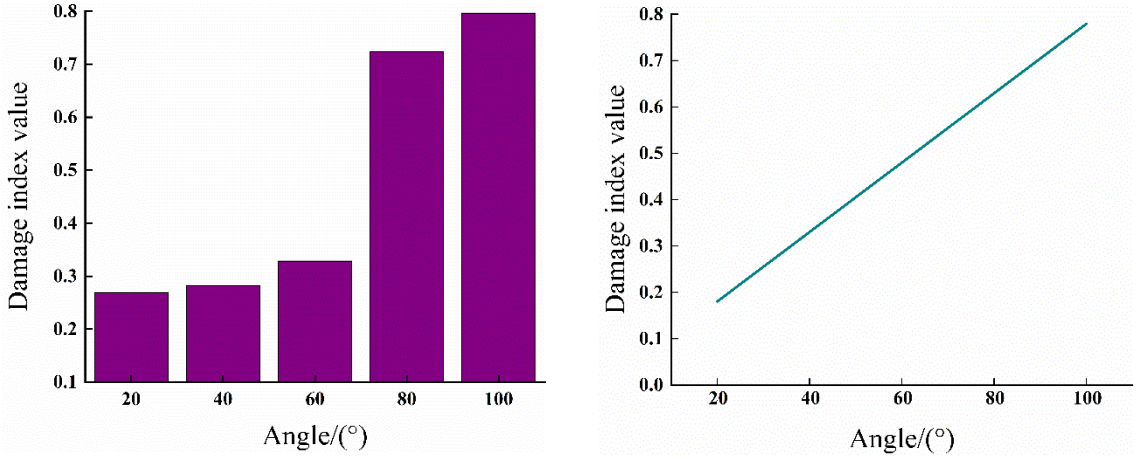
Damage reflection wave arrival time	0.521×10^{-4}s	0.514×10^{-4}s	0.530×10^{-4}s	3.02%	3.02%

Table 4. Comparison of finite element simulation results of pipeline structure propagation velocity

Comparative Analysis of Damage Index Values Under Different Operating Conditions

1) Influence of Damage Center Angle on Damage Index

Under fixed conditions of surface roughness, radial depth, and axial width, the variation trend of damage index values was analyzed as the circumferential damage center angle increased. Noise reduction and wavelet packet decomposition were applied to the sensor signals of each model under operating condition X. Signal energy was extracted from each node subset, and damage indices were calculated for each operating condition. Based on the obtained damage indices, a damage index matrix was constructed, as shown in Figure 7(a). The figure reveals that the damage index exhibits a monotonically increasing trend with increasing damage center angle.



(a) X damage index value (b) X Linear fitting curve

Figure 7. X1-X5 damage index matrix and linear fitting curve

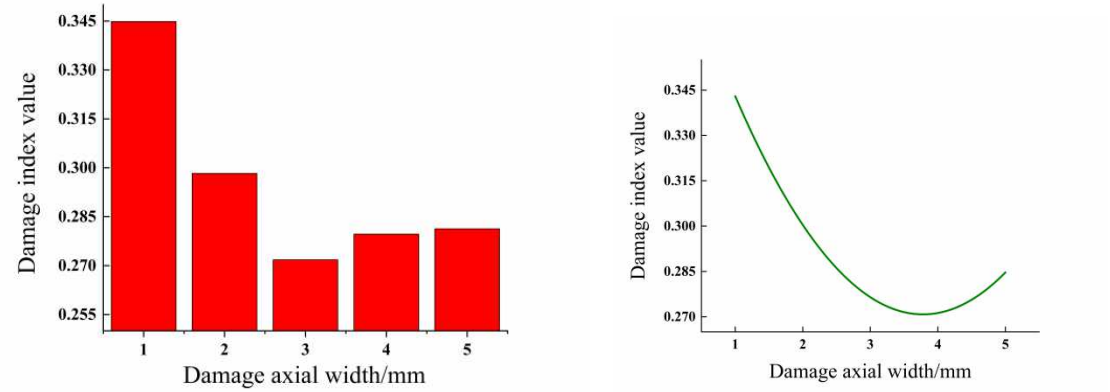
To quantify the relationship between the damage circle center angle and the damage index, a linear fitting relationship was established with the damage circle center angle as the independent variable and the damage index value as the dependent variable. The expression is $y = 0.00008334x^2 - 0.00251x + 0.26388$. The specific curve is shown in Figure 7(b). Further analysis of the damage index matrix reveals that the damage index value increases with the damage circular angle, exhibiting a significant jump within the circumferential damage circular angle range of 60° to 80°. This phenomenon indicates that damage may exert a discontinuous influence on guided wave propagation within this critical range. To investigate this mechanism further, subsequent studies may introduce denser operating conditions within this range for comparative analysis.

This principle aligns closely with the physical mechanism of guided wave propagation within pipeline structures. In non-destructive testing, the circumferential extent of a defect is the key geometric parameter determining its interaction intensity with guided waves. The circumferential extent of damage directly correlates with both the cross-sectional loss in the pipeline and the scattering intensity of guided waves. Circumferential damage with a larger

center angle generates a higher reflection coefficient during guided wave propagation, resulting in greater energy loss due to reflection, scattering, and mode conversion. This increased energy dissipation is more prominently reflected in the time-frequency characteristics of the piezoelectric sensor signal, leading to a higher damage index through algorithmic analysis. In their seminal work on pipeline guided wave detection, Cawley et al. [14] explicitly stated that the circumferential extent of a defect is the primary factor influencing the reflection coefficient, exerting a greater impact than the defect depth. Experimental and simulation results by Wang et al. [3] also indicate that as the circumferential coverage of a circular defect increases, the interaction area between the guided wave and the defect expands, leading to greater energy scattering or reflection. This results in higher amplitude anomalies in the sensor's received signal. Following wavelet packet decomposition, damage features become more pronounced in the time-frequency domain, ultimately driving the damage index to rise continuously with increasing circumferential central angle. The revelation of these patterns provides critical theoretical support for the quantitative NDT of circumferential pipeline damage, enabling more precise assessment of pipeline damage severity through guided wave signals.

2) Effect of Axial Width on Damage Index

Under fixed conditions of surface roughness, radial depth, and center angle, the variation trend of damage index values with increasing axial width of circumferential damage was analyzed. Wavelet packet decomposition was applied to the sensor signals extracted from piezoelectric sensors for each model under operating condition Y, yielding damage indices for each condition. The damage index values for each condition were obtained using the same methodology. Analysis revealed that the damage index exhibits a non-monotonic trend, first decreasing and then increasing with increasing axial width.



(a) Y damage index value (b) Y Linear fitting curve

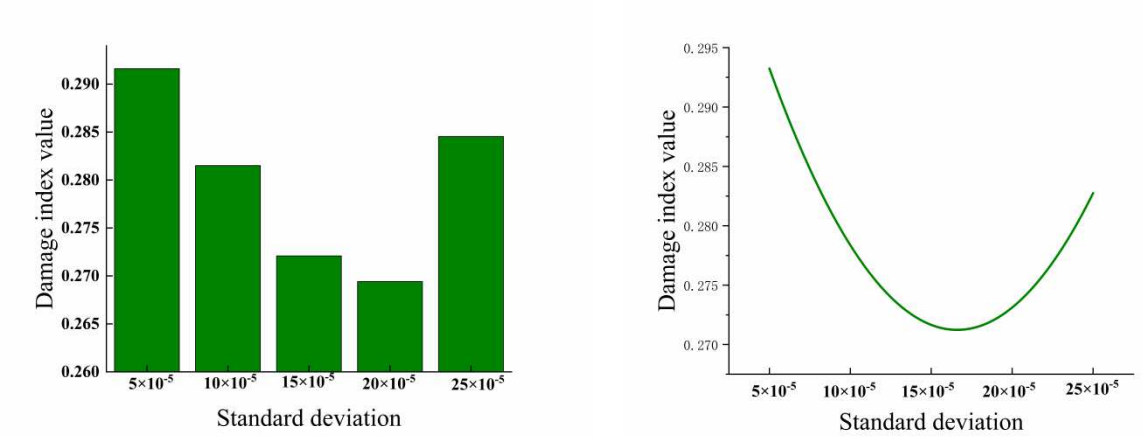
Figure 8. Y1-Y5 damage index matrix and linear fitting curve

As shown in Figure 8(a), this trend manifests as follows: when the axial width ranges from 1 mm to 3 mm, the damage index value exhibits a decreasing trend; when the axial width increases to the range of 3 mm to 5 mm, the trend reverses to an increasing one. To quantify the relationship between axial width and damage index, a fitting curve was established with axial width as the independent variable and damage index as the dependent variable. The expression is $y = 0.00934x^2 - 0.07063x + 0.40429$, as shown in Figure 8(b). revealing that the damage index reaches its minimum value within the 3 mm to 4 mm range.

The non-monotonic trend of the damage index decreasing then increasing with axial width can be explained by guided wave scattering theory. The mechanism is as follows: when the axial width of the damage matches the guided wave wavelength, the scattered waves generated at the front and rear edges of the defect undergo destructive interference, weakening the reflected echo energy and thereby reducing the damage index. This finding aligns with the conclusion reported by Demma et al. [15] that defects of specific dimensions can cause fluctuations in the reflection coefficient. Therefore, below a certain critical width, the destructive interference effect dominates, minimizing the measurable damage index. However, as the axial width of the defect continues to increase beyond this critical range, the blocking and scattering effects on wave propagation become predominant, causing the damage index to rise again.

3) Influence of Surface Roughness on Damage Index

Under fixed conditions of damage radial depth, circular angle, and axial width, the variation trend of damage index values with increasing surface roughness was analyzed. Wavelet packet decomposition was applied to the sensor signals extracted from piezoelectric sensors for each operating condition Z (roughness variable), yielding damage indices for each condition. The study revealed that the damage index exhibits a non-monotonic trend: it first decreases and then increases as the standard deviation of surface roughness increases.



(a) Z damage index value

(b) Z Linear fitting curve

Figure 9. Z1- Z5 damage index matrix and linear fitting curve

As shown in Figure 9(a), this trend manifests as follows: when the surface roughness standard deviation ranges from 5×10^{-5} to 20×10^{-5}, the damage index value exhibits a decreasing trend; when the damage roughness standard deviation ranges from 20×10^{-5} to 25×10^{-5}, it shows an increasing trend. To quantify the relationship between surface roughness and damage index values, a fitting curve was established with roughness standard deviation as the independent variable and damage index as the dependent variable. The expression for this curve is $y = 0.00409x^2 - 0.02714x + 0.3163$, as shown in Figure 9(b). Based on this fitting curve, the damage index reaches its minimum value within a roughness standard deviation range of approximately 15×10^{-5} to 20×10^{-5}.

Wave scattering and energy attenuation caused by surface roughness have been extensively studied in acoustic non-destructive testing [16]. Similarly, in this detection, surface roughness dominates scattering behavior, leading to non-monotonic variations or even attenuation of signal amplitude. At lower roughness levels, increased surface irregularities primarily enhance wave scattering, causing the damage index value to rise. However, when

roughness reaches a critical threshold (in this study, between 15×10^{-5} and 20×10^{-5}), the height variations of the rough surface induce diffuse scattering effects. This disperses acoustic energy across a wide spatial direction, reducing the energy returning to the sensor along the original path and consequently lowering the damage index value.

These results indicate that using traditional ideal smooth models while neglecting surface roughness may overestimate or underestimate the true detectability of actual rough damage. In contrast, the parametric roughness model established in this paper more accurately quantifies the mechanism by which damage affects guided waves. This improvement provides a critical theoretical model correction and basis for developing high-precision quantitative assessment algorithms for pipeline damage.

Conclusions

1. Trend Detection and Damage Identification Based on Damage Index: In actual operating conditions, pipeline damage typically evolves as a time-varying process. By continuously monitoring the trend (increasing or decreasing) of damage index values at adjacent time points, the severity of damage can be assessed. The fitted relationship established in this study between the damage index and key parameters provides a quantitative tool for this dynamic damage assessment. When the three parameters—radial depth, axial width, and roughness—are fixed, the damage index increases with the damage circular angle. This indicates that the trend in the damage index can enable damage assessment of rough corrosion surfaces using the damage circular angle as a variable.
2. Damage assessment and trend prediction based on non-monotonic variation patterns: The damage index fitting curve derived from the relationship between circumferential damage axial width, roughness, and the damage index reveals that the damage index first decreases then increases with increasing circumferential damage axial width and roughness. It achieves minimum values at 3mm-4mm and a standard deviation between 15×10^{-5} and 20×10^{-5}, respectively. Based on the damage index fitting curve with the roughness damage level of the pipeline structure, damage severity can be rapidly identified, and its development trend can be predicted. This study utilizes the finite element software ABAQUS to establish a soil–pipe interaction model. Consider the performance differences between undamaged and third-order corroded pipelines. By analyzing both reverse fault and normal fault positions in combination with different corrosion locations, jointly infer the performance analysis and failure modes of buried steel pipelines under normal fault conditions. On this basis, the failure modes of pipelines with stepped corrosion at different corrosion stages are further investigated. Stepped corrosion is driven by the simultaneous evolution of three parameters: corrosion depth (h/t), corrosion width (w), and corrosion length (l). The purpose of this investigation is to more realistically capture the damage induced by the actual corrosion process.

Data Availability Statement:

The datasets generated and analyzed during the current study are available from the corresponding author on reasonable request.

References

1. Zhao Manquan, Li Xiafei, Liu Fei, et al. Development and application status of T (0,1) modal guided wave detection technology in pipelines[J]. Technical Acoustics, 2019, 38(06): 632-639. DOI: 10.16300/j.cnki.1000-3630.2019.06.006.
2. Du Guofeng, Cheng Chen, Jiao Wenshuai, etc. Damage identification of pipelines based on piezoelectric ceramic sensors [J]. Journal of Yangtze University (Natural Science Edition), 2021,18 (02): 109-117.DOI: 10.16772 / j. cnki.1673-1409.2021.02.015.
3. Wang Xiaochu, Qu Lingzhi, Li Ying. Finite Element Simulation for Damage Degree Identification of Liquid - Filled Complex Pipeline Structures[J]. Journal of Shenyang University (Natural Science Edition), 2024, 36(04): 358 - 363 + 368. DOI: 10.16103/j.cnki.21 - 1583/n.2024.04.011.
4. PAN S S，XU Z D，LI D S，et al． Research on detection and location of fluid－filled pipeline leakage based on acoustic emission technology［J］． Sensors (Basel，Switzerland)，2018，18(11): 3628．
5. LANG X M，HU Z Y，LI P，et al． Pipeline leak aperture recognition based on wavelet packet analysis and a deep belief network with ICR［J］． Wireless Communications and Mobile Computing，2018，2018: 1－8．
6. Liu Bin, Feng Qibo, Kuang Cuifang.Review of surface roughness measurement methods [J]. Optical instruments, 2004, (05): 54-58.
7. Liang Xuequan, Lv Zhiyang, Xiao Shixuan, et al. Finite element analysis of contact sealing performance of oil and gas pipeline plugging fixture [J/OL]. Lubricating and sealing, 1-9 [2025-04-19]. https://kns-cnki-net.webvpn.cidp.edu.cn/kcms/detail/44.1260.TH.20250317.1038.018.html.
8. Cui Ximing, Wang Zhe, Zhang Zhuo, et al. Effect of surface roughness on piezoelectric ultrasonic thickness measurement [J]. Nondestructive testing, 2016,38 (05): 1-4.
9. Cebeci T, Cousteix J. Modeling and computation of boundary - layer flows [M]. Long Beach: Horizons Publishing Inc., 2005.
10. Wang Xiaochu, Qu Lingzhi, Li Ying. Finite element simulation of damage identification of layered pipeline structures based on damage index matrix [J]. Earthquake engineering and engineering vibration, 2023,43 (03): 189-197.DOI: 10.13197 / j. eeed.2023.0319.
11. Youngbin L, Sangyul H. 2023. “RufGen: A plug-in for rough surface generation in Abaqus/CAE.” [J]. SoftwareX,2023,22
12. ANSI/ASME B46.1-2019, Surface Texture (Surface Roughness, Waviness, and Lay) [S].
13. He Binbin. Damage Identification of Pipeline Structures Using PZT-Based Guided Waves[D]. Liaoning: Shenyang Jianzhu University, 2012.
14. Cawley P, Lowe S J M, Alleyne N D, et al. Practical long range guided wave testing: applications to pipes and rail[J]. Materials evaluation,2003,61(1):66-74.
15. Demma A, Caw1ey P, Lowe M. The reflection of guided waves from notches in pipes: a guide for interpreting corrosion measurements[J]. NDT & E international: Independent nondestructive testing and evaluation,2004,37(3):167-180.
16. Luc Kazandjian; Comparison of the Rayleigh–Fourier and extinction theorem methods applied to acoustic scattering in a waveguide. J. Acoust. Soc. Am. 1 November 1991; 90 (5): 2623–2627. https://doi.org/10.1121/1.402065.

Funding

This study was funded by the Spark Program of Earthquake Sciences.

Author Contributions

Conceptualization, Y. L.; Methodology, Ying LI and. Z.C.C.; Software, Z.C.C.; Validation, Z.C.C; Formal Analysis, Z.C.C.; Investigation, Y. L; Resources, Y. L.; Data Curation, Y. L.; Writing – Original Draft Preparation, Z.C.C.; Writing – Review & Editing, Y. L; Visualization, Z.C.C.; Supervision, Y. L.; Project Administration, Y. L.; Funding Acquisition, Y. L. All authors have read and agreed to the published version of the manuscript.

Conflicts of Interest

The authors declare no conflicts of interest.